COMPARATIVE INSILLICO STUDIES ON PHYTOCHEMICALS OF OCIMUM AS NATURAL INHIBITORS OF EBOLA VP-35 PROTEIN

Srinidhi Kashyap[*]

Department of Biotechnology, Ramaiah Institute of Technology, Bangalore, Karnataka, India.

ARTICLE INFO	ABSTRACT
	Ebola is a deadly single-stranded negative-sense RNA virus capable of causing hemorraghic fever and death in human and non-human primates. Ebola outbreaks worldwide have claimed a staggering 28000 lives and this virus could be used as a bioweapon for its high rate of transmission and fatality. Most importantly, the virus is unreceptive to a wide range of antiviral drugs and therapies. VP-24, VP-30, VP-35, and VP-40 are some of the important structural proteins of Ebola. VP-35 is a multifunctional structural protein of EBOLA and is crucial for its life processes. Exhaustive data-mining and literature survey was used to identify all the phytochemicals of the genus *Ocimum* and the control ligands against VP-35. Gossypetin, Gummosin, Limonin, and Taxifolin were the identified control ligands. ADME-TOX screening was employed to screen and shortlist phytochemicals for insillico studies. Comparative molecular docking simulation of the screened phytochemicals was performed primarily using iGEMDOCKv2.1 and further redocking simulation was performed using AutoDock Vina. Insillico studies on the 60 drug-likeness screened ligands yielded Cosmosiin (-7.2 kcal/mol), Molludistin (-7.1 kcal/mol) and Isovitexin (-7 kcal/mol) from *Ocimum* as the best ligands against VP-35. The control ligands were ranked as follows, Gummosin (-7.8 kcal/mol), Taxifolin (-7 kcal/mol), Gossypetin (-7 kcal/mol) and Limonin (-6.9 kcal/mol). Summarizing the results, Cosmosiin and Molludistin have superior binding affinities with VP-35 than 75% (3 out of 4) of the studied control ligands and these top-ranked phytochemicals of *Ocimum* identified could be used as efficient plant-based drug candidates to short-circuit the drug development phase and develop potent inhibitors against VP-35.

Corresponding author
Srinidhi Kashyap
Department of Biotechnology,
Ramaiah Institute of Technology,
Bangalore, Karnataka, India.
msrinidhi2@gmail.com

INTRODUCTION

Ebola is a deadly viral disease caused by a member of the family filovirideae. It is known to cause hemorrhagic fever leading to death. It is an endemic type of fever outbreak disease showing features of rapid spread like that of the plague caused by *Yarsinnia pestis* [1]. Ebola virus (EBOV) is a linear, negative-sense, enveloped, filamentous ribovirus known to occur in five types or species namely (Zaire, Sudan, Taï Forest, Bundibugyo and Reston Ebola virus) [2]. The outbreak is unsustainable to any underdeveloped country with a poor economic structure. As of 2016, there have been approximately 28000 confirmed cases including deaths [3]. The most recent outbreak of EBOV was in West Africa claiming a large number of lives and was very expensive, costing around 3 billion dollars. The structural and functional proteins of Ebola are coded by a total of seven genes found in the 19 kb long EBOV genome. The genome codes for proteins VP-35, VP-40, VP-24, VP-30, glycoprotein (GP1 and GP2 Dimer) and nucleoprotein responsible for effecting all processes associated with the viral life cycle [4]. The Glycoprotein (GP1 - GP2 heterodimer), VP-35 and VP-40 proteins are found in large quantities compared to the other structural proteins [3]. VP-35 forms complexes with other viral proteins to elicit important functions like the formation of the viral nucleocapsid, as a cofactor to viral polymerase domain and also acts as an antagonist to host antiviral interferon production [5]. VP-35 inhibits host interferon production (IFNα/β) for host immune evasion by interacting with RIG-1 and MDA-5 by direct contact with TBK-1 and IKKε) and by sequestration of dsRNA. Therefore, VP-35 can serve as a potential target for designing and developing drugs against EBOV as it contributes significantly to the virulence and pathogenicity of the virus.

Indian medicinal practices incorporate the use of a variety of plant materials to treat a vast number of diseases and ailments. Plants like *Asparagus racemosus*, *Curcuma longa, Azadirachta indica, Momordica charantia, Elettaria cardamom, Syzygium aromaticum* and members of the genus *Ocimum* are widely used to possess antiseptic, anti-microbial, anti-inflammatory, immunity enhancers, bio-enhancers and most importantly anti-viral properties [6][7][8]. The phytochemicals from members of the genus Ocimum of family Lamiaceae could be studied for the possibility of screening them for potential inhibitory activity against VP-35 of the Ebola virus using an in-Silico approach [9]. The prime objective of the present investigation is to identify phytochemical inhibitors of viral VP-35 protein from compounds of genus *Ocimum* by *insillico* methods by comparing the obtained results with previously identified and established phytochemical inhibitors of VP-35. The identified phytochemicals could serve as leads for drug design and development against EBOV during massive outbreaks in underdeveloped countries.

MATERIALS AND METHODS.
Identification of chemical space.

The members of the genus Ocimum were obtained from the online database *The Plant List* [10]. Phytochemicals of the listed species were retrieved from the Knapsack metabolite activity database [11] and Dr. Duke's phytochemical and ethnobotanical database [12]. A total of 85 phytochemicals were shortlisted from the databases by an extensive literature survey [7], [8], [13]–[20]. A literature survey was also conducted to identify phytochemical control ligands for analytical comparison and for scaffolding the obtained docking results in this study. The Phytochemicals, Gossypetin, Taxifolin, Limonin and Gummosin were identified by literature survey and were used as control ligands in this work [9], [21].

Evaluation of drug-like properties.

Pharmacokinetic and pharmacological parameters of all the 85 listed phytochemicals were computed using the admetSAR module [33] and the swissADME tool [34]. The initial screening and elimination of all the mined phytochemicals was done based on Lipinski's rule of 5 (RO5) as the acceptance criteria [35]. The bioavailability radar representation of the shortlisted phytochemicals was also obtained from swissADME [34]. The structures of the shortlisted phytochemicals were drawn using ChemDrawUltra 9.0 [36]. The molecules that qualified ADMET properties and drug-like attributes were further subjected to molecular docking studies.

Preparation of ligands.

The 3-D structure of the shortlisted phytochemical test and control ligands were obtained from the PubChem database. The ligands were then subjected to energy minimization and structural optimization using the minimize structure tool of UCSF chimera 1.13.1 suite [22]. The minimize structure tool in UCSF Chimera 1.13.1 suite entails structural minimization using 100 steepest descent steps with a step size of 0.02 Å and 10 conjugate gradient steps with a step size of 0.02 Å, polar hydrogens, and Gasteiger partial charges were added and the resulting prepared ligands were saved in mol2 and pdbqt formats for docking studies. The inter-conversion of file types was done using the OpenBabel GUI converter [23]

Preparation of the receptor protein.

The crystal structure of the VP-35 was retrieved from the protein data bank [24]. PDB CODE : 4IBF , the structure had a co-crystallized ligand ((4-{(2R)-2-(4-bromothiophen-2-yl)-3-[(5-chlorothiophen-2-yl)carbonyl]-4-hydr oxy-5-oxo-2,5-dihydro-1H-pyrrol-1-yl}phenyl)acetic acid (three-letter code: 1D5) (formula: C21H13BrClNO5S2)) at the active site , which was useful for binding site identification on the protein ,also the retrieved 3-D structure of the enzyme had a resolution of 2.291 Å, which was optimum for this study . The 4IBF-VP-35 structure was experimentally solved by x-ray crystallography, proving that the protein contains 48% alpha helices and 13 % beta-sheet as the secondary structures. The protein is dimeric, containing two chains annotated as A and B, with 129 residues each [25], [26].

The Chimera suite was used to remove the co-crystallized 1D5 ligand in the interferon inhibitory site of the protein. 'Dock Prep' tool of UCSF Chimera 1.13.1 suite [22] was used for the preparation of the VP-35 protein for molecular docking. Dock prep tool was used to add Incomplete side chains using the Dunbrack 2010 rotamer library. Polar hydrogens were added and water molecules were removed, Gasteiger partial charges were added. Receptor energy minimization was carried out by using a default constraint of 0.3Å RMSD (root mean square) and AMBER force field. The prepared structure was saved in .pdbqt format.

Identification of VP-35 binding site.

The binding site residues and grid coordinates of the VP-35 protein for docking analysis was identified by literature survey and visualization using PyMol 2.3.2 [27]. The grid coordinates of the VP-35 binding site was narrowed down to (41.281 * 19.745 * 57.587). Protein visualization and literature survey were used to identify the binding site residues of VP-35. The VP-35 binding site was found to be constituted with the following residues, Ala-221, Arg-225, Gln-241, Leu-242, Lys-248, Lys-251, Pro-293, Pro-292, Ile-295, Ile-297, His-296, Asp-302, Phe-328 Ala-238, Val-245, Ile-246, LEU-249, Ile-278, Ile-280, Phe-287, Ala- 306, Cys-307, Pro-315, Pro-318, Ile-320, Asp-321, Gly-323, Trp- 324, Val-325, Leu-338 and Ile-340 [3], [5], [23] All these residues together constitute 47 binding pockets of the Interferon inhibitory domain, polymerase cofactor activity site and other binding sites for protein-protein complex formation [9]. The binding site of VP-35 is represented in Fig 1.

Molecular docking simulation.
Primary docking simulation-IGEMDOCK.

Docking simulation of the ADME-T screened ligands was performed using the iGEMDOCK-v2.1 docking module [29]. iGEMDOCK employs a generic evolutionary method algorithm to perform integrated screening, docking, and post-analysis. The binding site preparation tool in iGEMDOCK was used to specify the binding site of the VP-35 protein [30]. The software requires .pdb format for both protein and ligand inputs. Other parameters like population size, generations, and the number of solutions were set to 800, 80 and 10 respectively for accurate docking. The scoring function of iGEMDOCK can be illustrated as follows;

$$\text{Fitness} = \text{vdW} + E_{\text{Hydrogen bond}} + E_{\text{Electrostatic}}$$

Where, vdW is Vander waal's energy (kcal/mol), H-bond is hydrogen bond energy (kcal/mol) and Elec is electrostatic forces (kcal/mol) between the ligand and receptor protein [31].
The post-analysis of the docked poses was performed by the interaction profile tool in iGEMDOCK. The fitness, Vander waal's forces, hydrogen bond energy, electrostatic force energy, and interacting residues were obtained and tabulated [28]. Top eight compound hits were selected based on overall fitness and H-bond energies for further redock studies. .

Redocking simulation-AutoDock-Vina.

Redocking analysis was performed using the AutoDock vina tool in UCSF Chimera suite 1.13.1 [22] for a comprehensive comparative analysis. AutoDock vina uses a scoring function illustrated as follows;

$$C = C_{\text{inter}} + C_{\text{intra}}$$

Where, 'C' stands for molecular contributions.
The software tries to find the global minimum of this function to rank the ligand-receptor complexes. AutoDock Vina employs a robust gradient optimization method in its local optimization procedure. By this method of optimization, Vina gains a sense of direction during the scoring and ranking process after each evaluation [32]. The top ligand hits obtained from post-analysis of the primary docking simulation performed using iGEMDOCK v2.1 [29] was redocked into the same receptor for comparative docking analysis using AutoDock Vina tool in UCSF Chimera 1.13.1 suite [22]. The binding site grid co-ordinates were set, Ligand and receptor charges were merged, non-polar hydrogens were removed, exhaustiveness of search was fixed to 8 and maximum energy of 3kcal/mol was considered. The top scores and associated docked poses were analyzed, the interacting residues were identified, tabulated and summarized in Table 3. The top-scored docked poses were exported to PyMol 2.3.2 [27] for visualization, analysis and pictorial representation.
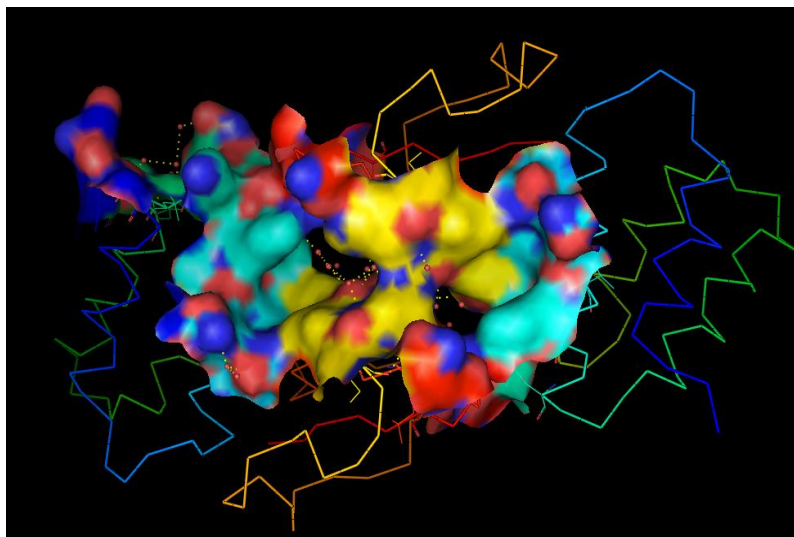
Fig 1: Pictorial representation of surface view of VP-35 binding site.

RESULTS AND DISCUSSION.
Pharmacokinetic screening.

A total of 75 metabolites were screened for various parameters pertaining to physicochemical properties like absorption, distribution, metabolism, elimination of the compounds. Deviation from Lipinski's Rule of five was used as the filter to screen phytochemicals with acceptable drug-likeness properties. 60 metabolites showed acceptable drug-likeness properties. The phytochemicals violating one rule of Lipinski have also been considered for further study. The ADME parameters of the 60 phytochemicals are depicted in Table 1. These ligands were further studied for their binding affinity to VP-35 by molecular docking studies.

Molecular docking analysis.

Molecular docking studies of the 4 control ligands and 60 ADME screened phytochemical compounds from ten species of the genus *Ocimum* namely, *Ocimum americanum, Ocimum basilicum, Ocimum gratissimum, Ocimum kilimandscharicum, Ocimum lamiifolium, Ocimum rubrum, Ocimum sanctum, Ocimum spicatum, Ocimum spp* and *Ocimum x citriodorum* was carried out primarily using iGEMDOCK v2.1 to find out the binding free energy, energy split-up as well as the interactions of the ligands with the active site residues of the VP-35 protein. The test ligands were ranked based on their hydrogen bond energies and the top eight test ligands were chosen for redock simulation. The results of primary docking simulation are summarized in Table 1. Among the studied ligands, Isovitexin (*Ocimum sanctum*) and cosmosiin (*Ocimum sanctum*) were ranked in the first and second place with total binding energies of -107.096 kcal/mol and -98.094 kcal/mol, respectively. The hydrogen bond energies ranged from -20.2315 kcal/mol and -18.8651 kcal/mol, respectively. Isovitexin showed hydrogen bond interactions with Lys-222, Arg-225, Val-294, and His-296. The interactions of Isovitexin with Arg-225 and His-296 are noteworthy, because these residues constitute the interferon inhibitory domain of the VP-35. Cosmosiin shared two significant hydrogen bond interactions with IID residues His-296 and Ile-297, respectively. Molludistin was found to interact with His-296, Gln-329, Leu-330, Lys-248 and Gln-331, respectively. Interactions of molludistin with the main chains of Lys-248 and His-296 can be highlighted because studies show that ligand interactions with Lys-248 results in complete loss of compound binding and complex formation ability of VP-35 with L protein and nucleoprotein leading to failure of different processes in the viral life cycle [25]. The remaining ligands Apigenin, Luteolin, D-Mannuronic acid, Xanthomicrol and Hydroxy-3',4',6,7-Tetramethoxyflavone also showed prominent hydrogen bond interactions with important binding site residues like Ile-297, Ile-295, Gln-244, Lys-248. The binding energies ranged from -81.288 kcal/mol to -108 kcal/mol. The ligand hits also had hydrophobic, polar and nonpolar interactions with Gln-331, Leu-330, Lys-222, Val-243, Gln-224, Asp-252, Leu-330, Gln-331 and Val-245 in a 3Å radius around the active site of the VP-35. The binding energies of the control ligands, Gossypetin, Gummosin, Taxifolin and Limonin (ranked in that order) displayed total binding energies ranging from -86.59 kcal/mol to -93 kcal/mol. Likewise, hydrogen bond energies ranging from -3.41 kcal/mol to -28.39 kcal/mol, respectively. The docking simulation of the control ligands was performed for the sake of comparative analysis of the binding energies between the test and control compounds. Gossypetin displayed interactions with His-296, Leu-330, Gln-331, Gln-244 and Val-245. The interactions of gossypetin with His-296 and Gln-244 are noteworthy as they constitute the key binding residues of the VP-35 interferon inhibitory domain (IID). Furthermore, Taxifolin displayed several interactions with Asp-218, Lys-251, Asn-254, Ser-255, Leu-256, and Asp-257. Interaction of taxifolin with Lys-251 is prominent among others as it is crucial for the polymerase cofactor function of the VP-35 protein. Protein structural studies show that alterations and mutations of the Lys-251 residue leads to loss of function of the viral polymerase activity leading to viral life cycle arrest and attenuation [5], [25].

Table 1: Primary docking results illustrating total binding energy, energy split up and interacting residues of control and test ligands.

		CONTROL LIGANDS					
		PRIMARY DOCKING ANALYSIS					SPECIES
RANK	COMPOUND NAME	TOTAL BINDING ENERGY kcal/mol	VANDER WALL'S ENERGY kcal/mol	HYDROGEN BOND ENERGY kcal/mol	ELECTR OSTATIC BOND ENERGY kcal/mol	INTERACTING RESIDUES	
1	Gossypetin	-92.9068	-74.7467	-18.1601	0	HIS-296, LEU-330, GLN-331, GLN244, VAL-295	*Hibiscus sabdariffa*
2	Gummosin	-90.2122	-75.7695	-14.4427	0	HIS-296, VAL-295	*Ferula gummosa*
3	Taxifolin	-88.1841	-59.7911	-28.393	0	ASP218, LYS-251, ASN-254, SER-255, LEU-256, ASP-257,	*Cedrus deodara*
4	Limonin	-86.5912	-83.1751	-3.41609	0	VAL-295	*Citrus Medica*
		PHYTOCHEMICAL LIGANDS OF OCIMUM					
		PRIMARY DOCKING ANALYSIS					SPECIES
RANK	COMPOUND NAME	TOTAL BINDING ENERGY kcal/mol	VANDER WALL'S ENERGY kcal/mol	HYDROGEN BOND ENERGY kcal/mol	ELECTR OSTATIC BOND ENERGY kcal/mol	INTERACTING RESIDUES	
1	Isovitexin	-107.096	-86.865	-20.2315	0	LYS-222, ARG-225, VAL-295, HIS-296	*Ocimum sanctum*
2	Cosmosiin	-98.0943	-79.2292	-18.8651	0	HIS-296, ILE-297	*Ocimum sanctum*
3	Molludistin	-91.4825	-65.1652	-26.3173	0	HIS-296, GLN-329, LEU-330, LYS-248, GLN-331	*Ocimum sanctum*
4	Xanthomicrol	-87.58	-67.23	-20.35	0	GLN-244, VAL-245, VAL-294, HIS-296	*Ocimum americum*
5	Luteolin	-86.39	-63.58	-22.82	0	GLN-244, VAL-245, HIS296,	*Ocimum americum*
6	Apigenin	-83.71	-55.95	-27.76	0	LYS-222, ARG-225, VAL-243, GLN-224ASP-252	*Ocimum americum*
7	Hydroxy-3',4',6,7-Tetramethoxyf lavone	-81.2886	-62.2046	-19.084	0	LYS-248, HIS-296	*Ocimum americum*
8	D-Mannuronic acid	-77.848	-51.2129	-22.5553	-4.0798	VAL-294, HIS-296,	*Ocimum Basilicum*

Redock analysis was performed on the eight ligands that were filtered out from the 60 screened compounds during primary docking. Results of the redocking simulation are summarized in Table 2. Among the eight compounds studied, Cosmosiin (Fig 3-b) was ranked in the first place with -7.2 kcal/mol. Interactions of cosmosiin with Gln-241 and His-296 are notable among others as these two residues are nested in the active site (IID) of VP-35. Molludistin (Fig3-f) was ranked in second place with a binding energy of -7.1 kcal/mol. Also, molludistin showed hydrogen bond interactions with important binding site residues like His-296, Gln-241, and Lys-248. We can speculate potential antagonistic viral polymerase cofactor activity from Molludistin due to its interaction with Lys-248, an important active site residue associated with viral polymerase co-factor activity of VP-35 [25], [37]. Lastly, the best-docked

Page 502

pose of Isovitexin (Fig 3-c) in the binding site was ranked in the third place with a binding energy of -7 kcal/mol. Isovitexin was found to interact with important binding site residues like His-296, Lys-248, and Gln-244.

It Is evident that the top three compound hits of both primary and redocking simulation are the same Viz Cosmosiin, Molludistin, and Isovitexin. It is also noteworthy to observe that the binding energies of Cosmosiin and molludistin are better than three of the four control ligands. Also, the binding energy of Isovitexin (3rd rank and -7 kcal/mol) was found to be equal to two of the control ligands (Gossypetin and Taxifolin) (Fig 2-a, d) and superior than Limonin (4th rank and -6.9 kcal/mol) (Fig 2-c).

Table 2: Redocking results illustrating the individual ranks and scores, interacting residues and sources of control and test ligands.

RANK	COMPOUND NAME	SCORE (kcal/mol)	INTERACTING RESIDUES	SPECIES
CONTROL LIGANDS				
		REDOCKING ANALYSIS		
1	Gummosin	-7.8	GLN-241, HIS-296, ILE-295	*Ferula gummosa*
2	Taxifolin	-7	GLN-331, HIS-296, GLN-244	*Cedrus deodara*
3	Gossypetin	-7	HIS-296, ILE-295, GLN-244, GLN-331, THR-335	*Hibiscus sabdariffa*
4	Limonin	-6.9	LYS-251, GLN-244	*Citrus Medica*
PHYTOCHEMICAL LIGANDS OF OCIMUM				
		REDOCKING ANALYSIS		
1	Cosmosiin	-7.2	GLN-241, HIS-296, GLN-329	*Ocimum sanctum*
2	Molludistin	-7.1	HIS-296, GLN-241, LYS-248	*Ocimum sanctum*
3	Isovitexin	-7	HIS-296, LYS-248, GLN-244	*Ocimum sanctum*
4	Apigenin	-6.9	GLN-241, GLN-329, HIS-296, GLN-331	*Ocimum americum*
5	Luteolin	-6.9	HIS-296, GLN-244, ILE-246	*Ocimum americum*
6	Hydroxy-3',4',6,7-Tetramethoxyflavone	-6.3	GLN-244, GLN-241, HIS-296	*Ocimum americum*
7	Xanthomicrol	-6	ARG-225, GLN-244, VAL-294	*Ocimum americum*
8	D-Mannuronic acid	-4.7	HIS-296	*Ocimum Basilicum*
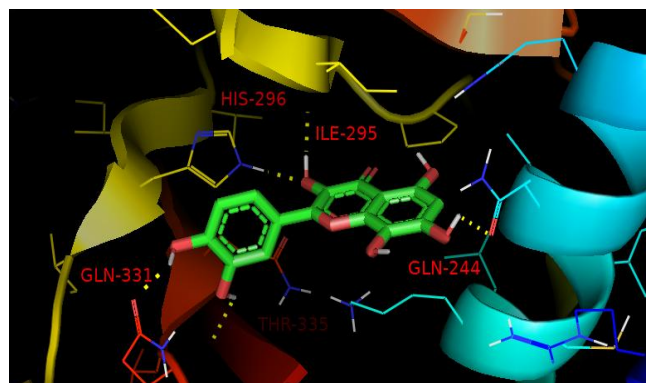
Gossypetin-A
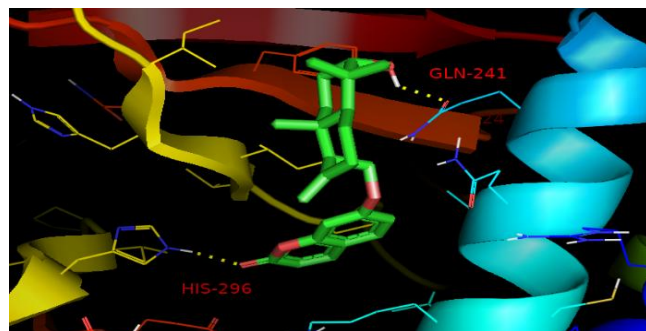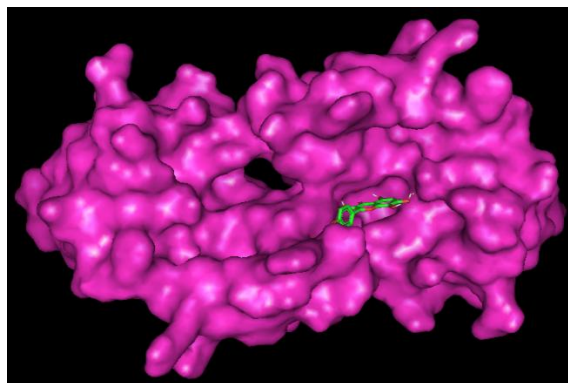
Gummosin-B
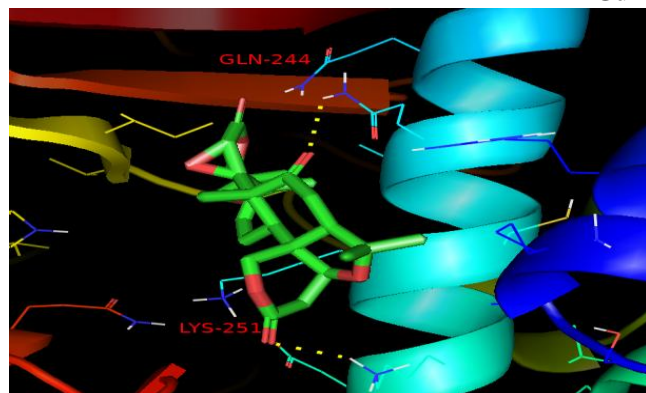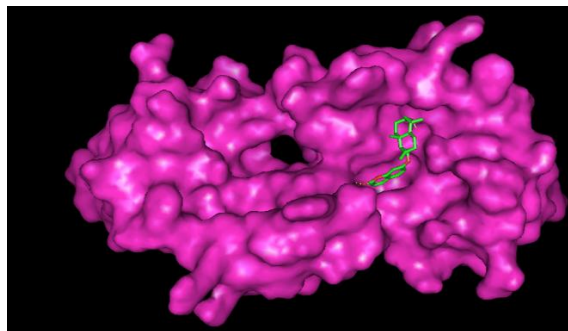
Limonin-C
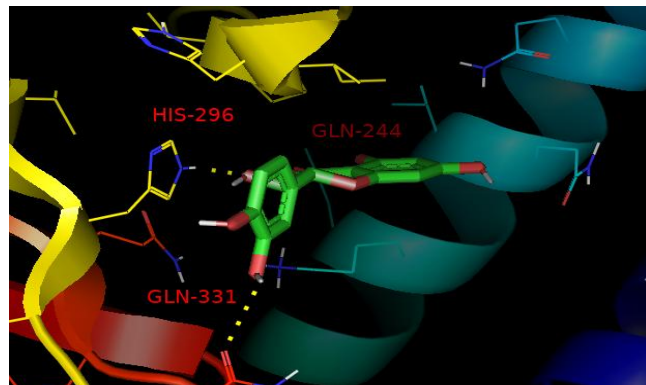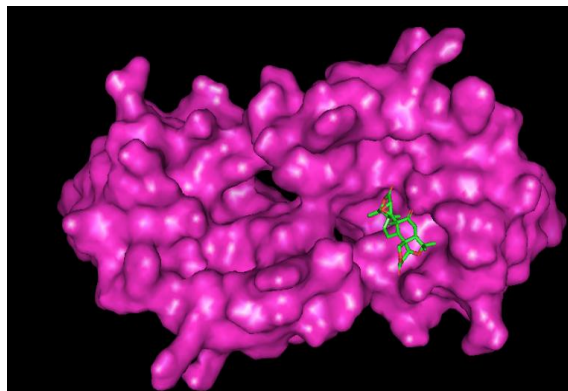
Taxifolin-D
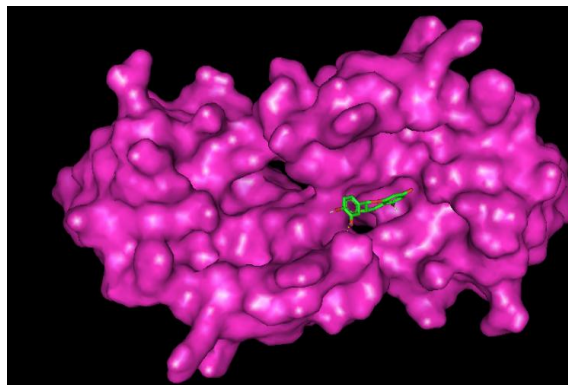
Fig 2 (a-d): Pictorial representation of Ligand-protein residue interactions and surface view of the docked control ligands in VP-35 binding site.
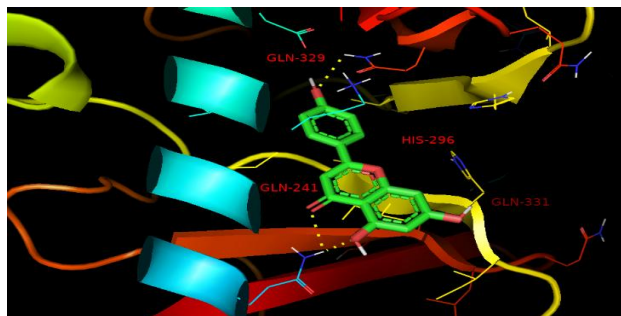
Apigenin-A
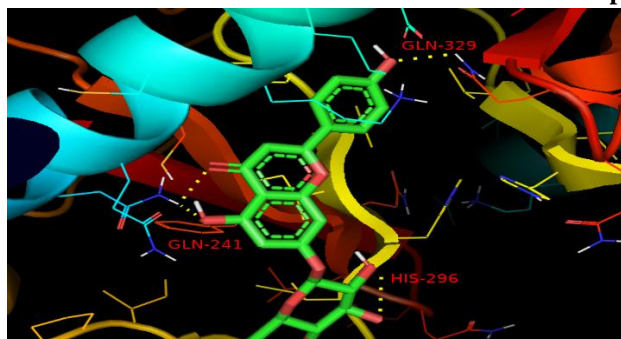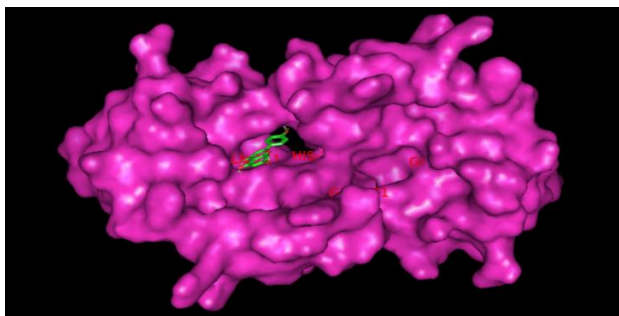
Cosmosin-B
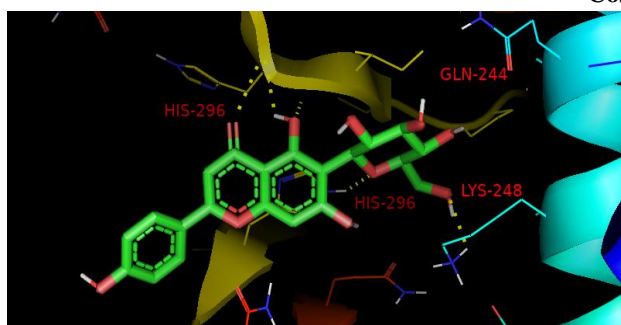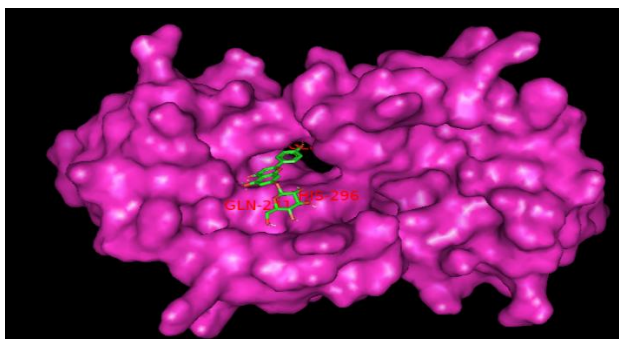
Isovitexin-C
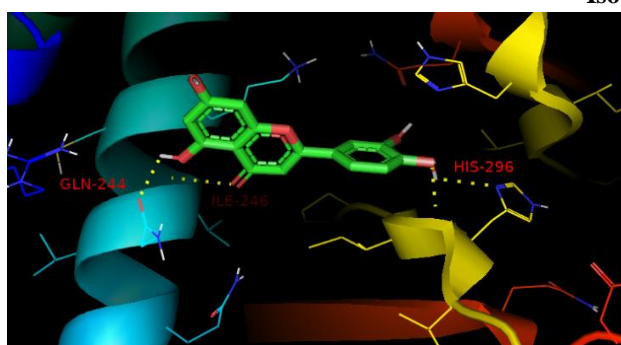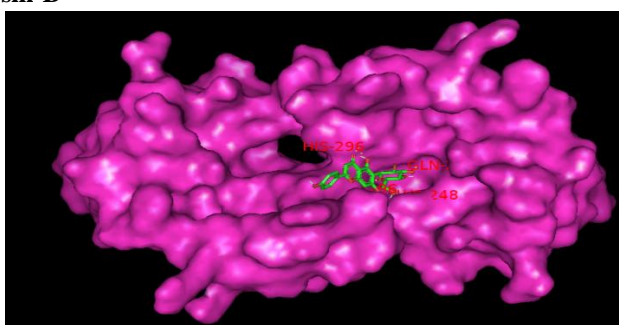
Luteolin-D

Mannuronic Acid-E

Page 505
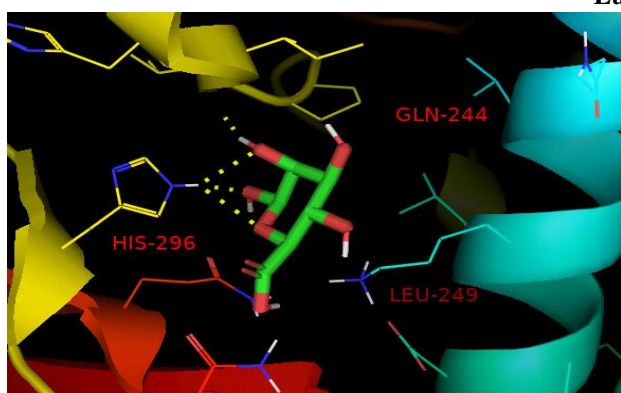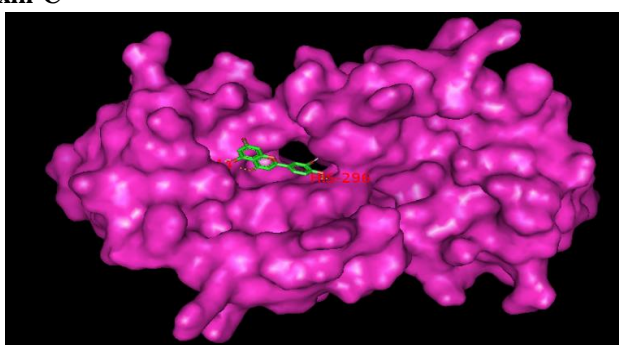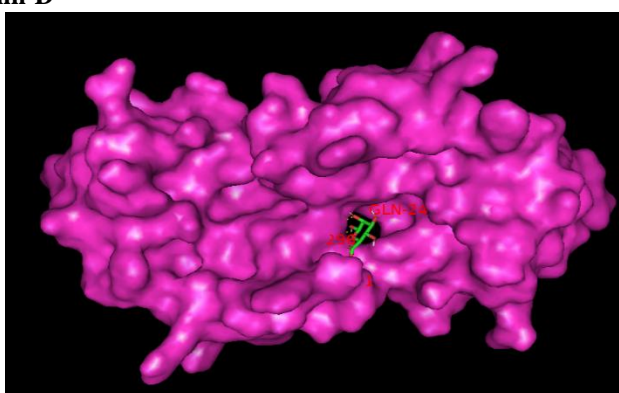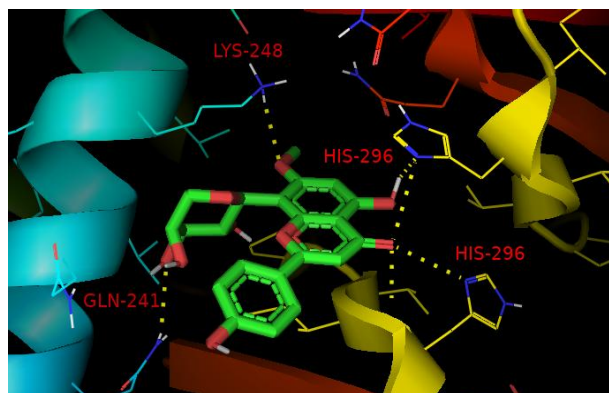
Molludistin-F
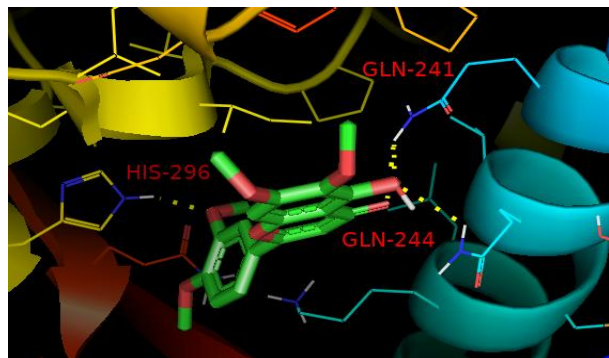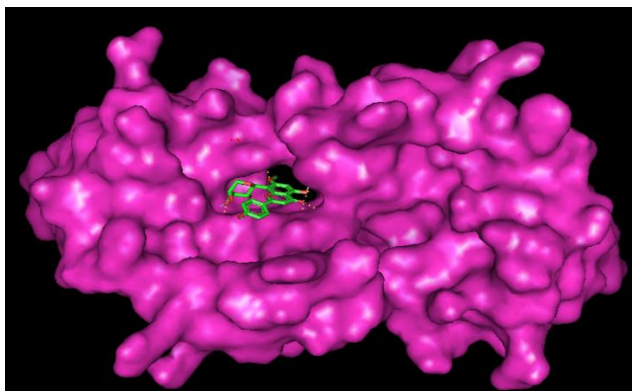
Tetramethoxy Flavone-G
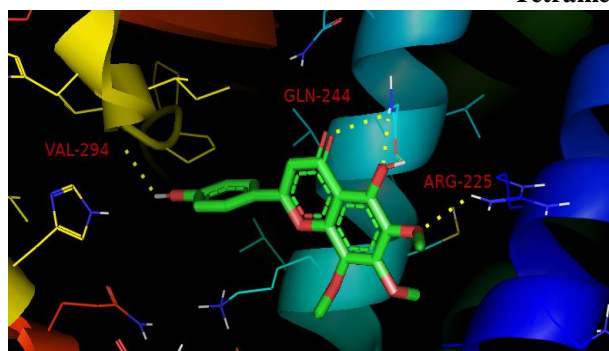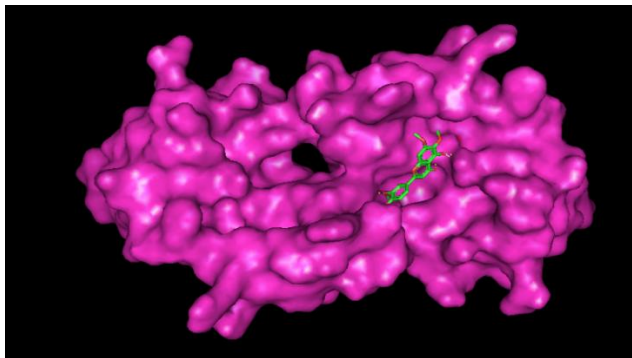
Xanthomicrol-H
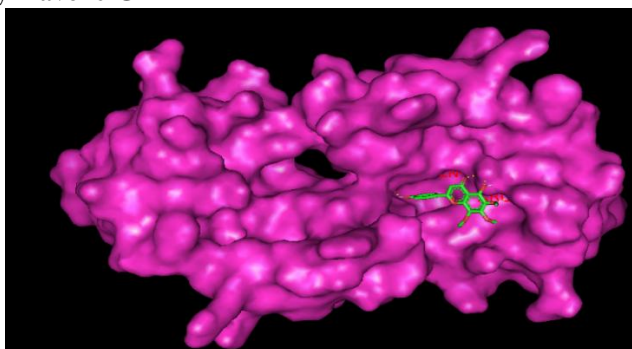
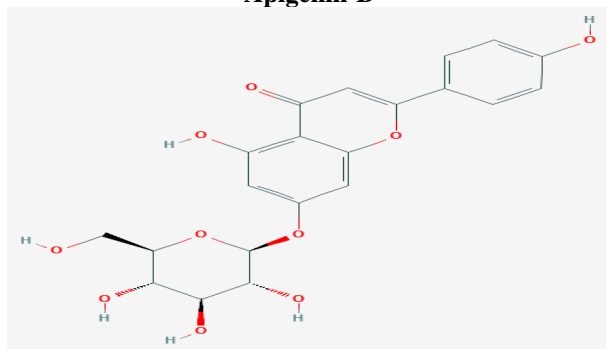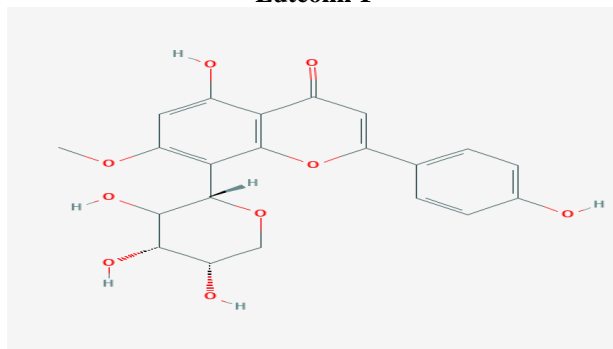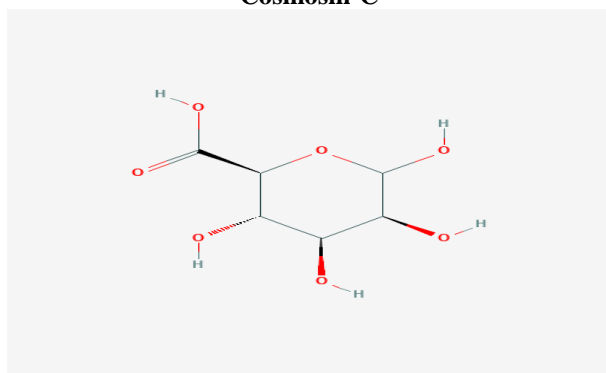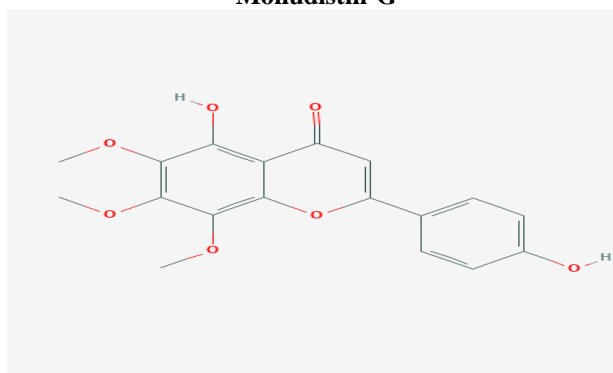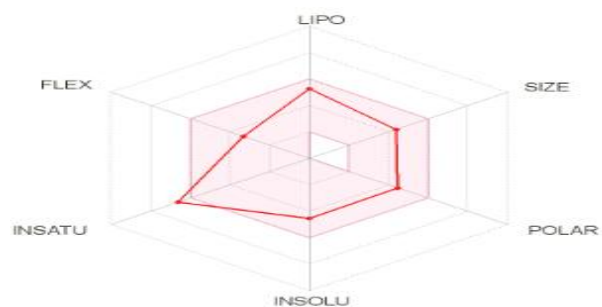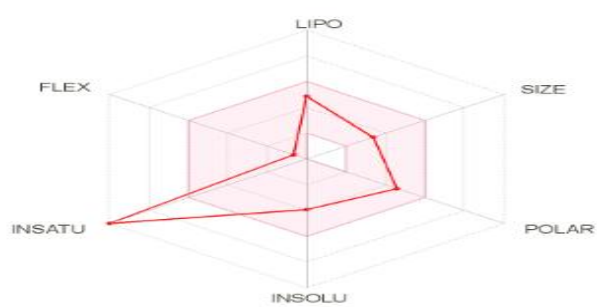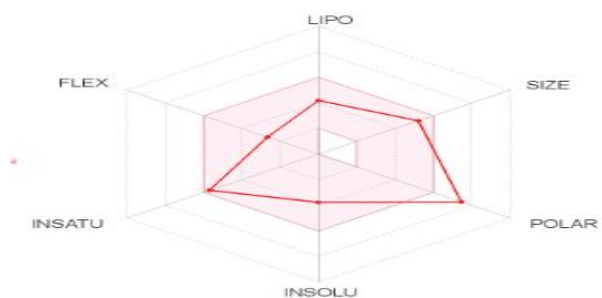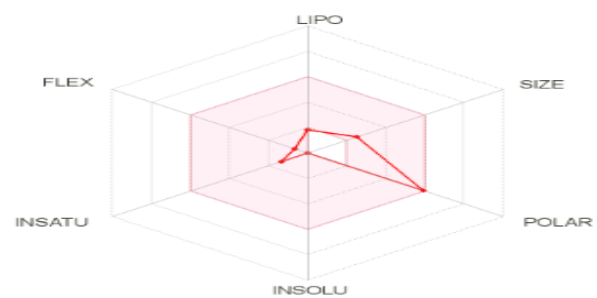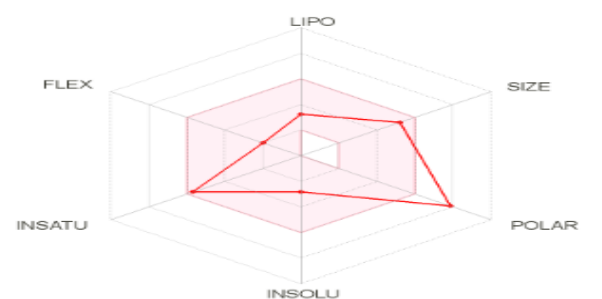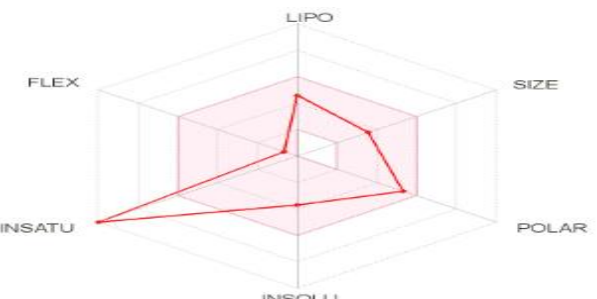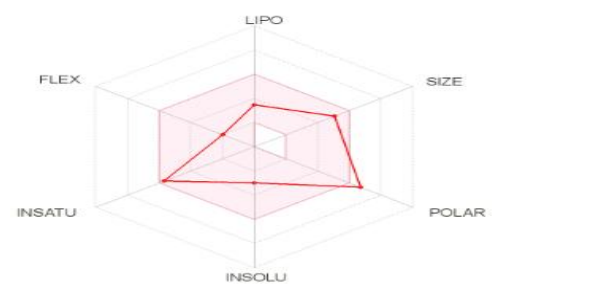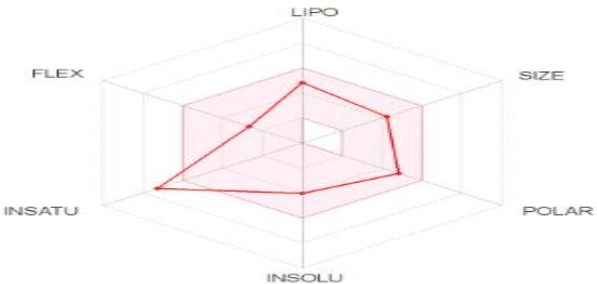**Fig 3 (a-h): Pictorial representation of Ligand-protein residue interactions and surface view of docked test ligands in VP-35 binding site.**

Druglikeness assessment of the hit compounds.

The Swiss-ADME tool was employed to procure the bioavailability radar illustrations of the test and control ligand hits from redocking analysis. The bioavailability radars of the compounds are depicted in the Table 1. Six drug-likeness parameters namely, INSATU (unsaturation), INSOLU (Insolubility), LIPO (LogP), FLEX (Rotatable Bonds), SIZE (Molecular weight) are POLAR (Polar surface area) of each compound are concisely illustrated in their respective radars. The pink region of the radar depicts the optimum region for each of these five properties [38]. Upon analysis, it was found that the Control ligands followed the following decreasing trend of druglikeness, Gummosin > Limonin > Taxifolin > Gossypetin. The structures and bioavailability radar illustrations of the control ligands are depicted in (Fig 4 (a-d)). The radars of Taxifolin and Gossypetin were found to be similar with respect to their increased polar surface areas. On the other hand, Gummosin and Limonin were found to have similar bioavailability radars. The top three compound hits displayed the following decreasing trend of druglikeness, Molludistin > Cosmosiin > Isovitexin. The bioavailability radar illustrations of the test compounds are depicted in (Fig 6 (a-h)). The polar surface area of Molludistin, Cosmosiin, and Isovitexin were little outside the optimum region (Pink-region) of the radars (decreasing in that order). All the other four drug-likeness parameters of the remaining compounds were well within the optimum region. Furthermore, among the other five compounds, all the parameters were well within the optimum value except for a slight increase in their polar surface areas.

Page 506
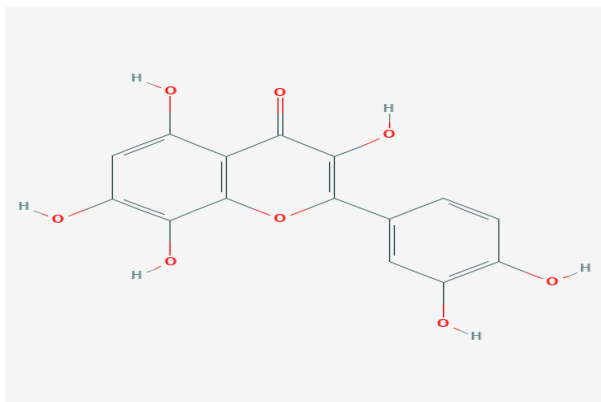
Gossypetin-A
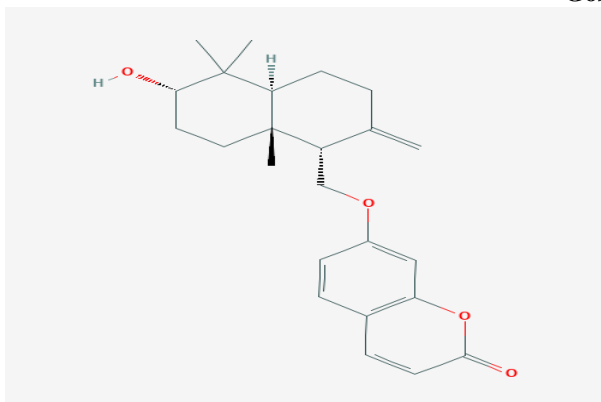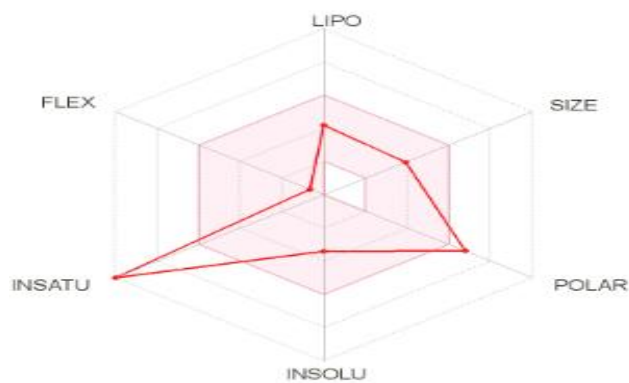
Gummosin-B
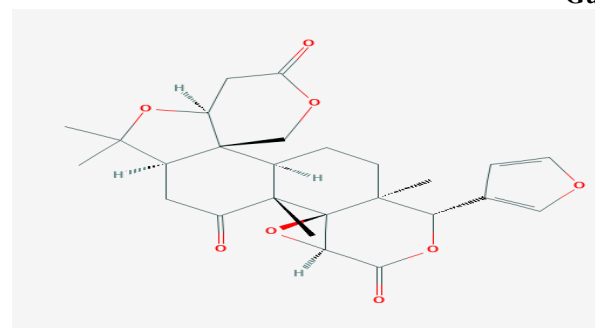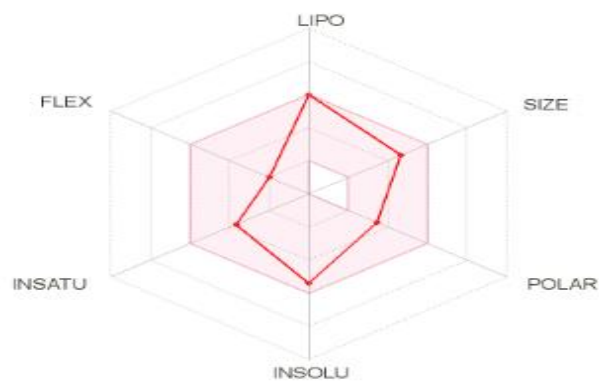
Limonin-C
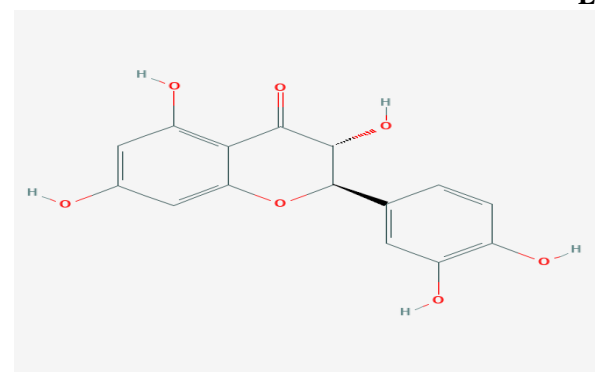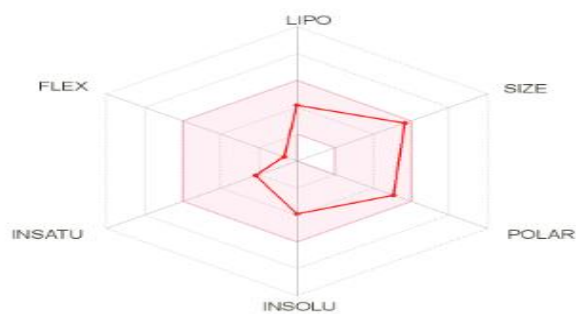
Taxifolin-D
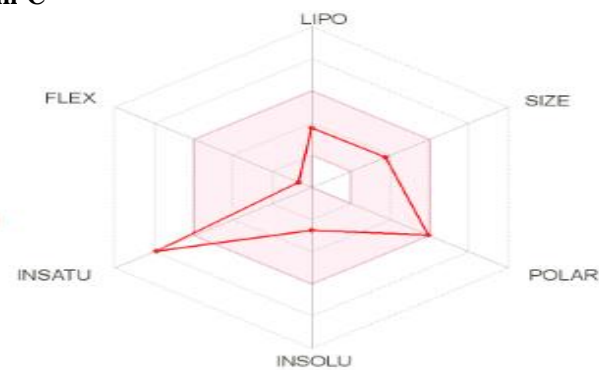
Figure 4 (a-d): Pictorial representation of structures and bioavailability radar illustrations of control ligands.
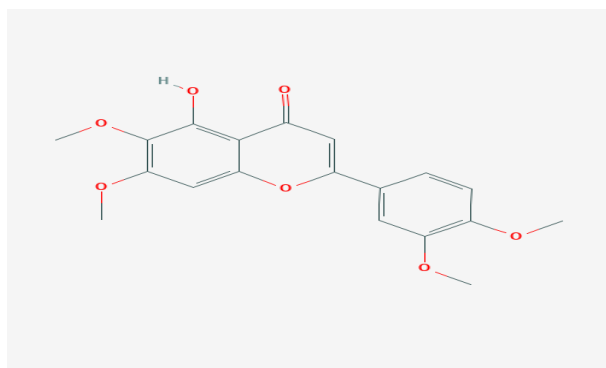
5-Hydroxy-3',4',6,7-Tetramethoxyflavone-A
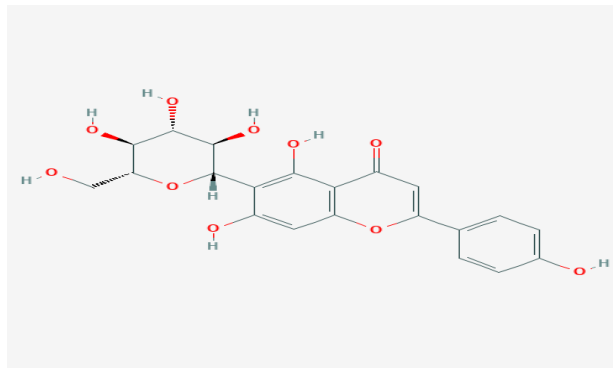
Isovitexin-E
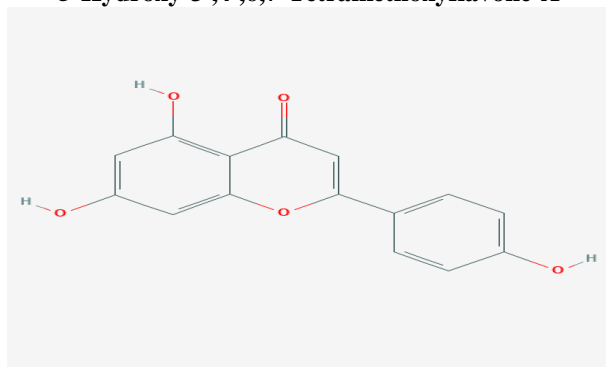
Apigenin-B
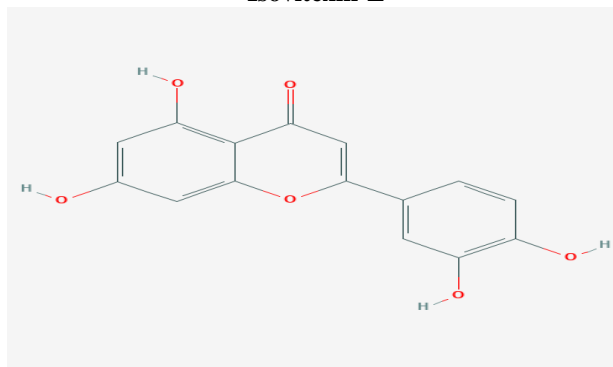
Luteolin-F

Cosmosin-C

Molludistin-G

D-Mannuronic Acid-D

Xanthomicrol-H

Figure 5 (a-h): Pictorial representation of structures of test ligands.

5-Hydroxy-3',4',6,7-Tetramethoxyflavone-A

Apigenin-B

Cosmosiin-C

D-Mannuronic Acid-D

Isovitexin-E

Luteolin-F

Molludistin-G

Xanthomicrol-H

Figure: 6 (a-h): Pictorial representation of bioavailability radars of test ligands.

CONCLUSIONS

Based on the results obtained from this study, the following conclusions were drawn.

- Cosmosiin, Molludistin, and Isovitexin from *Ocimum sanctum* were the best compound hits among the studied compounds.
- From the different interactions exhibited by these three compounds with the binding site residues of the VP-35 protein. It can be inferred that these compounds upon binding with VP-35 would structurally alter and completely inhibit various functions of the viral protein leading to its attenuation.

Page509

FUTURE SCOPE

Molecular dynamics simulation, Invitro and in vivo cytotoxicity studies, Estimation of IC50 values of individual and a mixture of these compounds against different types of infected cell lines would unequivocally prove the efficacy of these compounds against Ebola. Furthermore, based on the results obtained after performing the previously mentioned studies on these compounds, A decoction or solvent-based extract of *Ocimum Sanctum, Ocimum americium,* and *Ocimum basilicum* could be used as a supplementary therapeutic aid for treating Ebola similar to how Papaya (*Carica papaya*) is used to treat Dengue fever [39] .

CONFLICT OF INTEREST

There are no conflicts of interest regarding this work and this study has not received any financial support.

ACKNOWLEDGMENTS.

REFERENCES.

1. S. N. Mali and H. K. Chaudhari, "Molecular modelling studies on adamantane-based Ebola virus GP-1 inhibitors using docking, pharmacophore and 3D-QSAR," *SAR QSAR Environ. Res.*, vol. 30, no. 3, pp. 161–180, 2019.
2. J. S. Richardson, J. D. Dekker, M. A. Croyle, and G. P. Kobinger, "Recent advances in Ebolavirus vaccine development," *Hum. Vaccin.*, vol. 6, no. 6, pp. 439–449, 2010.
3. M. U. Mirza and N. Ikram, "Integrated computational approach for virtual hit identification against ebola viral proteins VP35 and VP40," *Int. J. Mol. Sci.*, vol. 17, no. 11, Nov. 2016.
4. A. Grifoni *et al.*, "Genetic diversity in Ebola virus: Phylogenetic and in silico structural studies of Ebola viral proteins," *Asian Pac. J. Trop. Med.*, vol. 9, no. 4, pp. 337–343, Apr. 2016.
5. D. W. Leung, K. C. Prins, C. F. Basler, and G. K. Amarasinghe, "Ebolavirus VP35 is a multifunctional virulence factor," *Virulence*, vol. 1, no. 6, pp. 526–531, 2010.
6. I. Ahmad and A. Z. Beg, "Antimicrobial and phytochemical studies on 45 Indian medicinal plants against multi-drug resistant human pathogens," *J. Ethnopharmacol.*, vol. 74, no. 2, pp. 113–123, 2001.
7. V. Gaddaguti, T. Venkateswara Rao, and A. Prasada Rao, "Potential mosquito repellent compounds of Ocimum species against 3N7H and 3Q8I of Anopheles gambiae," *3 Biotech*, vol. 6, no. 1, pp. 1–8, Dec. 2016.
8. P. Gupta, D. K. Yadav, K. B. Siripurapu, G. Palit, and R. Maurya, "Constituents of Ocimum sanctum with antistress activity," *J. Nat. Prod.*, vol. 70, no. 9, pp. 1410–1416, Sep. 2007.
9. A. S. Setlur, S. Y. Naik, and S. Skariyachan, "Herbal Lead as Ideal Bioactive Compounds Against Probable Drug Targets of Ebola Virus in Comparison with Known Chemical Analogue: A Computational Drug Discovery Perspective," *Interdiscip. Sci. Comput. Life Sci.*, vol. 9, no. 2, pp. 254–277, 2017.
10. "The Plant List," *version 1.1*, 2013. [Online]. Available: http://www.theplantlist.org/. [Accessed: 01-Jan-2019].
11. Y. Nakamura *et al.*, "KNApSAcK metabolite activity database for retrieving the relationships between metabolites and biological activities," *Plant Cell Physiol.*, vol. 55, no. 1, Jan. 2014.
12. U.S. Department of Agriculture, "Dr. Duke's Phytochemical and Ethnobotanical Databases," *Agricultural Research Service*. [Online]. Available: https://phytochem.nal.usda.gov/.
13. Reshma, K. P. Arun, and P. Brindha, "In vitro anti-inflammatory, Antioxidant and nephroprotective studies on leaves of Aegle marmelos and Ocimum sanctum," *Asian J. Pharm. Clin. Res.*, vol. 7, no. 4, pp. 121–129, 2014.
14. A. Anand *et al.*, "Comparative functional characterization of eugenol synthase from four different Ocimum species: Implications on eugenol accumulation," *Biochim. Biophys. Acta - Proteins Proteomics*, vol. 1864, no. 11, pp. 1539–1547, Nov. 2016.
15. M. Pola, S. B. Rajulapati, C. Potla Durthi, R. R. Erva, and M. Bhatia, "In silico modelling and molecular dynamics simulation studies on L-Asparaginase isolated from bacterial endophyte of Ocimum tenuiflorum," *Enzyme Microb. Technol.*, vol. 117, pp. 32–40, Oct. 2018.
16. H. A. Bhatti *et al.*, "Identification of new potent inhibitor of aldose reductase from Ocimum basilicum," *Bioorg. Chem.*, vol. 75, pp. 62–70, 2017.
17. M. M. Arkajyoti Paul, Mohammad Shah Hafez Kabir, Mir Muhammad Nasir Uddina and M. R. H. Rahmana, Abul Hasanata, Tanvir Ahmad Chowdhury, Md. Nazim Uddin Chy, "Anticancer potential of isolated phytochemicals from Ocimum sanctum against breast cancer: In silico Molecular docking approach," vol. 5, no. 12, pp. 1232–1239, 2016.
18. A. Ghasemzadeh, S. Ashkani, A. Baghdadi, A. Pazoki, H. Z. E. Jaafar, and A. Rahmat, "Improvement in flavonoids and phenolic acids production and pharmaceutical quality of sweet basil (Ocimum basilicum L.) by ultraviolet-B irradiation," *Molecules*, vol. 21, no. 9, Sep. 2016.
19. T. Bhavani *et al.*, "Phytochemical screening & antimicrobial activity of Ocimum gratissimum review," ~ 76 ~ *J. Pharmacogn. Phytochem.*, vol. 8, no. 2, pp. 76–79, 2019.
20. D. Singh and P. K. Chaudhuri, "A review on phytochemical and pharmacological properties of Holy basil (Ocimum sanctum

Page 510

L.),” *Ind. Crops Prod.*, vol. 118, no. March, pp. 367–382, 2018.

21. U. Raj and P. K. Varadwaj, “Flavonoids as Multi-target Inhibitors for Proteins Associated with Ebola Virus: In Silico Discovery Using Virtual Screening and Molecular Docking Studies,” *Interdiscip. Sci. Comput. Life Sci.*, vol. 8, no. 2, pp. 132–141, Jun. 2016.

22. F. TE Pettersen EF, Goddard TD, Huang CC, Couch GS, Greenblatt DM, Meng EC, “UCSF Chimera--a visualization system for exploratory research and analysis,” *J Comput Chem*, 2004.

23. N. M. O’Boyle, M. Banck, C. A. James, C. Morley, T. Vandermeersch, and G. R. Hutchison, “Open Babel: An Open chemical toolbox,” *J. Cheminform.*, vol. 3, no. 10, Oct. 2011.

24. H. M. Berman, “The Protein Data Bank / Biopython,” *Presentation*, vol. 28, no. 1, pp. 235–242, 2000.

25. C. S. Brown *et al.*, “In silico derived small molecules bind the filovirus VP35 protein and inhibit its polymerase cofactor activity,” *J. Mol. Biol.*, vol. 426, no. 10, pp. 2045–2058, May 2014.

26. L. H. Elliott, M. P. Kiley, and J. B. McCormick, “Descriptive analysis of Ebola virus proteins,” *Virology*, vol. 147, no. 1, pp. 169–176, 1985.

27. D. Seeliger and B. L. De Groot, “Ligand docking and binding site analysis with PyMOL and Autodock/Vina,” *J. Comput. Aided. Mol. Des.*, vol. 24, no. 5, pp. 417–422, 2010.

28. “Graphical-Automatic Drug Design System for Docking, Screening and Post-Analysis,” 2008.

29. J.-M. Yang and C.-C. Chen, “GEMDOCK: A Generic Evolutionary Method for Molecular Docking,” 2004.

30. B. Sathyamurthy and H. S. Sushmitha, “In Silico drug designing studies on Dengue Virus NS1 Protein,” *PharmaTutor*, vol. 6, no. 10, p. 31, Jan. 2018.

31. T. Khan, R. Ahmad, I. Azad, S. Raza, S. Joshi, and A. R. Khan, “Computer-aided drug design and virtual screening of targeted combinatorial libraries of mixed-ligand transition metal complexes of 2-butanone thiosemicarbazone,” *Comput. Biol. Chem.*, vol. 75, pp. 178–195, Aug. 2018.

32. O. Trott and A. J. Olson, “Software news and update AutoDock Vina: Improving the speed and accuracy of docking with a new scoring function, efficient optimization, and multithreading,” *J. Comput. Chem.*, vol. 31, no. 2, pp. 455–461, Jan. 2010.

33. F. Cheng *et al.*, “AdmetSAR: A comprehensive source and free tool for assessment of chemical ADMET properties,” *J. Chem. Inf. Model.*, vol. 52, no. 11, pp. 3099–3105, 2012.

34. A. Daina, O. Michielin, and V. Zoete, “SwissADME: A free web tool to evaluate pharmacokinetics, drug-likeness and medicinal chemistry friendliness of small molecules,” *Sci. Rep.*, vol. 7, Mar. 2017.

35. S. Celik, A. T. Albayrak, S. Akyuz, and A. E. Ozel, “Synthesis, molecular docking and ADMET study of ionic liquid as anticancer inhibitors of DNA and COX-2, TOPII enzymes,” *J. Biomol. Struct. Dyn.*, 2019.

36. K. R. Cousins, “ChemDraw Ultra 9.0. CambridgeSoft, 100 CambridgePark Drive, Cambridge, MA 02140. www.cambridgesoft.com. See Web site for pricing options.,” *J. Am. Chem. Soc.*, vol. 127, no. 11, pp. 4115–4116, Mar. 2005.

37. K. C. Prins, J. M. Binning, R. S. Shabman, D. W. Leung, G. K. Amarasinghe, and C. F. Basler, “Basic Residues within the Ebolavirus VP35 Protein Are Required for Its Viral Polymerase Cofactor Function,” *J. Virol.*, vol. 84, no. 20, pp. 10581–10591, 2010.

38. K. O. Sulaiman, T. U. Kolapo, A. T. Onawole, M. A. Islam, R. O. Adegoke, and S. O. Badmus, “Molecular dynamics and combined docking studies for the identification of Zaire ebola virus inhibitors,” *J. Biomol. Struct. Dyn.*, vol. 37, no. 12, pp. 3029–3040, 2019.

39. N. Ahmad, H. Fazal, M. Ayaz, B. H. Abbasi, I. Mohammad, and L. Fazal, “Dengue fever treatment with Carica papaya leaves extracts,” *Asian Pac. J. Trop. Biomed.*, vol. 1, no. 4, pp. 330–333, 2011.

5487847845119**1003**

Page 511